PROCEEDINGS OF THE CANADIAN SOCIETY FOR MECHANICAL ENGINEERING INTERNATIONAL CONGRESS 2023
CSME CONGRESS 2023
MAY 28-31, 2023, SHERBROOKE, QC, CANADA

MODEL PREDICTIVE CONTROL USING MACHINE LEARNING FOR VOLTAGE CONTROL OF A PEM FUEL CELL STACK

Sina Moghadasi[1*], Alireza Salahi[1], Hoseinali Borhan[2], Charles Robert Koch[1], Mahdi Shahbakhti[1]
[1]Department of Mechanical Engineering, University of Alberta, Edmonton, Canada
[2]Cummins Inc, Columbus, IN 47201, USA
[*]smoghada@ualberta.ca

***Abstract*—In this paper, a Nonlinear Model Predictive Control (NMPC) is designed using a data-based model of Proton Exchange Membrane Fuel cell (PEMFC) for output voltage control. To capture PEMFC complex dynamics and non-linearities, Machine Learning (ML) algorithms are utilized to model the behavior of the system. This model is then embedded inside the NMPC controller to provide the predictions required for solving the optimization problem. The NMPC not only provides precise output voltage tracking, but also can simultaneously reduce the fuel consumption of the stack as one additional term in the cost function. Moreover, the possible upper and lower bounds of the control effort generated by actuators are set as the hard constraints of NMPC. The simulation results show that while these constraints are not violated, the desired output voltage is generated with less fuel being consumed comparing to the case that fuel consumption is not controlled.**

***Index Terms*—Machine Learning Control, Proton-exchange membrane fuel cell, Minimizing fuel consumption, Model Predictive Control**

I. Introduction

In the recent decades, the need for a clean alternative for fossil fuels has motivated investing on renewable and carbon-free solutions. Accordingly, the Fuel Cell (FC) technology has proven to be one of the promising ways for producing power with less harmful environmental effects than the fossil fuels [1]. The FC technology comes in different types and designs that consume a variety of fuels including hydrogen, methane, ethanol, and methanol [2].

Among all types of fuel cells, Proton Exchange Membrane Fuel Cell (PEMFC) has demonstrated the highest power to volume ratio. Therefore, PEMFCs have been used in various stationary and mobile applications ranging from residential power generation to Fuel Cell Hybrid Electric Vehicles (FCHEV). Fig.1 shows a simple illustration of the PEMFC structure. PEMFC requires highly pure hydrogen as fuel. First, the hydrogen molecules are ionized at the anode. Then the hydrogen atoms travel through the proton-exchange membrane to the cathode side where they react with the oxygen molecules and produce water. Anode and cathode are connected with an external circuit for conducting the electrons by which the produced electric power is exploited. The chemical reactions inside PEMFC are described in Eq. (1) [3].

$$\begin{aligned} &\text{Anode: } H_2 \Rightarrow 2H^+ + 2e^- \\ &\text{Cathode: } O_2 + 4H^+ + 4e^- \Rightarrow 2H_2O \\ &\text{Overall reaction: } H_2 + 1/2O_2 \Rightarrow H_2O \end{aligned} \tag{1}$$

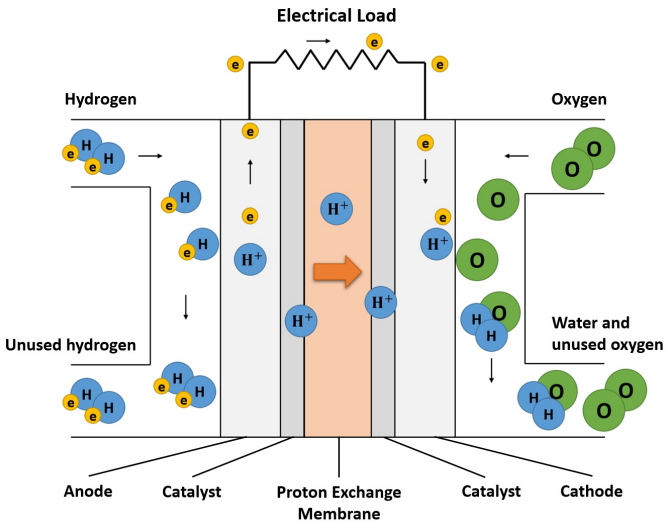

Fig. 1: Schematic of PEMFC operation

Typically, the output voltage of a single cell is not adequate for practical usage. Thus, many cells are connected together in parallel and series to form one fuel cell stack. The generated power of the stack is the first variable of interest which is mainly controlled by the fuel and air flow rates. Depending on the application of PEMFC, the output voltage is required to follow different patterns from a constant reference with focus on disturbance rejection to tracking fast voltage demands.

There have been significant research efforts regarding the control of PEMFC. Methekar et al. [4] designed a centralized Multiple-Input Multiple-Output (MIMO) controller for con-

trolling average output power and temperature by manipulating hydrogen and coolant flow rates. The oxygen flow rate is in a constant ratio with respect to the hydrogen flow that prevents the oxygen starvation. Pukrushpan et al. [5] followed the same approach to control fuel utilization and the temperature measured at catalyst using fuel flow and air flow. Gabin et al. [6] utilized single-input single-output (SISO) Sliding Mode Control (SMC) to prevent oxygen starvation by manipulating the input oxygen. In [7], Chatrattanawet et al. proposed a Model Predictive Control (MPC) to control the cell voltage and cell temperature using the flow rates of input hydrogen and air. Bordons et al. [8] also implemented MPC controller using a nonlinear model of PEMFC and prevented oxygen starvation with air flow control.

MPC is one of the effective methods for controlling PEMFC as it enables having an optimal solution for controlling all the desired variables by keeping the future behavior of the system in consideration. Furthermore, system and operational constraints can be introduced to the controller to avoid violating them as the PEMFC operates [9]. Nevertheless, the MPC requires a model of the system to solve the optimization problem over a prediction horizon. The PEMFC dynamic equations are highly nonlinear with several input and output variables that makes the control-oriented model computationally expensive. Hence, by using a data-driven model as the prediction model inside the NMPC, the computational cost will be mitigated substantially [10]. Therefore, machine learning methods are proposed as a solution for modeling the non-linear system of PEMFC based on input and output data. This model will be embedded in the MPC controller to provide required predictions of the system. To the best of authors' knowledge, this is the first study undertaken to use a data-driven model inside the NMPC to predict the output voltage of PEMFC.

The rest of the paper is organized as follows. Section II introduces the fundamental physics and specifications of the PEMFC system. Section III provides the details about collecting data from the system and designing a model using ML algorithms. In section IV, the designed model is used inside the MPC while the cost function and parameters of the MPC are mentioned. Finally, the results are reported in section V and section VI concludes the outcomes of the paper.

II. PEM Fuel Cell Plant Modeling

In this section, cardinal dynamic equations of PEMFC are proposed based on Nernst dynamic method [11]. After deriving the dynamic equations of the fuel-cell stack, the detailed Simulink model of a 6 kW stationary fuel-cell system will be designed including a 100 V-dc power generating circuit. The equation of fuel cell output voltage with associated losses at any time instance can be defined as: [11] [11]

$$V_{cell} = E_{fc} - V_{act} - V_{ohm} - V_{conc} \tag{2}$$

Where V_{act} indicates the activation voltage loss due to slowness of the chemical reactions on electrode surfaces, V_{ohm} is the ohmic loss caused by internal resistance of the fuel cell stack, V_{conc} shows the losses due to changes in concentration of reactants as the fuel is being used, and E_{fc} indicates the open loop circuit voltage of the system. Open loop voltage of the system can be calculated based on the Nernst dynamic equation as below [9]:

$$E_{fc} = \begin{cases} 1.229 + (\mathrm{T} - 298)\frac{-44.43}{\mathrm{zF}} + \frac{\mathrm{RT}}{\mathrm{zF}} \ln(P_{H_2} P_{O_2}^{\frac{1}{2}}) & \mathrm{T} \leq 100^{\circ}C \\ 1.229 + (\mathrm{T} - 298)\frac{-44.43}{\mathrm{zF}} + \frac{\mathrm{RT}}{\mathrm{zF}} \ln(\frac{P_{H_2} P_{O_2}^{\frac{1}{2}}}{P_{H_2O}}) & \mathrm{T} > 100^{\circ}C \end{cases} \tag{3}$$

Where T is the stack working temperature, z indicates the number of moving electrons, F shows the Faraday's constant, and R is the global gas constant. P_{H_2}, P_{O_2}, and P_{H_2O} indicate the equivalent pressure of hydrogen, oxygen, and water on the electrode surfaces, respectively. The values of constant parameters are provided in Table I. The activation drops which is obtained from the TOFEL equation can be expressed as [12]:

$$\begin{aligned} V_{act} &= 0.9514 - 3.12 \times 10^{-3}\,\mathrm{T} - 7.4 \times 10^{-5}\,\mathrm{T}_{O_2} \\ &+ 1.87 \times 10^{-4}\,\mathrm{T} \ln I \end{aligned} \tag{4}$$

Where I is the instantaneous current density in milli-ampere per square centimeter, and C_{O_2} is the oxygen concentration on the electrode surface which is calculated as a function of cell temperature [11]:

$$V_{O_2} = \frac{P_{O_2}}{5.08 \times 10^6 \exp(\frac{-498}{\mathrm{T}})} \tag{5}$$

Under low current densities, the stack losses can be represented by linear terms and can be described as ohmic loss [12]:

$$V_{ohm} = I\,(R_M + R_C) \tag{6}$$

$$R_M = \frac{\rho_M\, l}{\mathrm{A}} \tag{7}$$

$$\rho_M = \frac{181.6[1 + 0.03\frac{I}{\mathrm{A}} + 0.062(\frac{\mathrm{T}}{303})^2(\frac{I}{\mathrm{A}})^{2.5}]}{[\Psi - 0.634 - 3\frac{I}{\mathrm{A}}]\,\exp[4.18(\frac{\mathrm{T}-303}{\mathrm{T}})]} \tag{8}$$

In which R_C is the contact resistance to electron flow, and R_M is the resistance to proton transfer through the membrane which can be calculated from Eq. (7). ρM is the membrane specific resistivity and l is the membrane thickness. Ψ represents the specific coefficient based on the fuel cell membrane type, and A is the membrane active area. The constant value of mentioned parameters and their units are shown in Table 1. Under higher current densities, due to the limitation of mass transportation through the membrane, the cell potential is decreased considerably and can be described as [12]:

$$V_{conc} = -\mathrm{B} \ln(1 - \frac{I}{I_{max}}) \tag{9}$$

Where B is a constant depending on the type of fuel cell, and I_{max} is the maximum electrical current passing through the fuel-cell stack in ampere. To estimate the pressure of hydrogen, oxygen, and water vapor on anode and cathode surfaces for replacing in Eq. (4), the expressions below can

be considered [9]:

$$\begin{aligned} P_{H_2} &= (1 - U_{f_{H_2}}) x P_{fuel} \\ P_{H_2O} &= (w + 2y U_{f_{O_2}}) P_{air} \\ P_{O_2} &= (1 - U_{f_{O_2}}) y P_{air} \end{aligned} \tag{10}$$

Where x is the percentage of hydrogen in the fuel, y is the percentage of oxygen in the oxidant, and w is the percentage of water vapor in the oxidant. P_{fuel} indicates the absolute supply pressure of fuel in atmosphere, and P_{air} is the absolute supply pressure of air in atmosphere. $U_{f_{H_2}}$ and $U_{f_{O_2}}$ are the rates of conversion or utilization of hydrogen and oxygen, respectively and can be calculated as: [13] [9]

$$\begin{aligned} U_{f_{H_2}} &= \frac{60000\,\mathrm{R\,T\,N}\,I}{\mathrm{z\,F}\,P_{fuel}\,V_{fuel}\,x\%} \\ U_{f_{O_2}} &= \frac{60000\,\mathrm{R\,T\,N}\,I}{\mathrm{z\,F}\,P_{air}\,V_{air}\,y\%} \end{aligned} \tag{11}$$

Where N is the total number of cells.V_{fuel} and V_{air} indicate the flow rates of fuel and air in liter per minute. Moreover, the constant number of 60,000 in the numerator of Eq. (11) is used to convert liter per minute to cubic meter per second.

For implementing a model of the fuel-cell stack based on the dynamic equations which are represented so far, MATLAB hydrogen fuel-cell stack in the Simscape environment is adapted. All the stack design parameters are set based on NetStack-PS6 real model which are reported in Table I. The nominal Fuel Cell Stack voltage is 45V-dc and the nominal power is 6 kW [13]. To supply the required voltage of the fuel cell, a converter is loaded by a resistor–inductor circuit of 6 kW with a time constant of one second. Resistance and inductance quantities are set as 1.66 Ω and 1.66 H, respectively.

TABLE I: Fuel cell design parameters based on NetStack-PS6 real model [9]

Parameter	Symbol	Quantity
Faraday constant (C/mol)	F	96.485
Global gas constant (mol/k)	R	8.314
Maximum current (A)	I_{max}	225
Contact resistance Ω	R_c	0.07833
Membrane thickness (cm)	l	175×10^{-4}
Specific coefficient	ψ	23
Membrane active area cm^2	A	50.6
Stack nominal voltage (V)	V_{nom}	45
Boltzmann constant	B	0.016
Fuel composition (%)	x	99.95
Oxidant composition (%)	y	21
Water composition (%)	w	1
Air supply pressure (bar)	P_{air}	1
Total number of cells	N	65
Nominal stack efficiency (%)	η_{nom}	0.55
Stack nominal current (A)	I_{nom}	133.3

The output power and voltage of one stack containing 65 cells can be calculated as follows [11]:

$$\begin{aligned} V_{stack} &= V_{cell}\,\mathrm{N} \\ P_{stack} &= V_{stack}\,I \end{aligned} \tag{12}$$

By varying the instantaneous stack current from 0 to 225 A, the characteristic curves of the 6 kW fuel cell are obtained as shown in Fig. 2. According to the stack nominal voltage and current which are 45 V and 133.3 A respectively, the total number of cells and the nominal air-flow-rate ($V_{air(nom)}$) can be obtained as below [9]:

$$\mathrm{N} = \frac{2\,\mathrm{F\,V}_{nom}}{241.83 \times 10^3\,\eta_{nom}} = 65 \tag{13}$$

$$V_{air(nom)} = \frac{I_{nom}\,V_{air(max)}}{I_{max}} = 297\frac{lit}{min} \tag{14}$$

Where $V_{air(max)}$ is the maximum stack air-flow-rate which is considered as 500 liter per minutes, specifically for NetStack-PS6 real model [9]:.

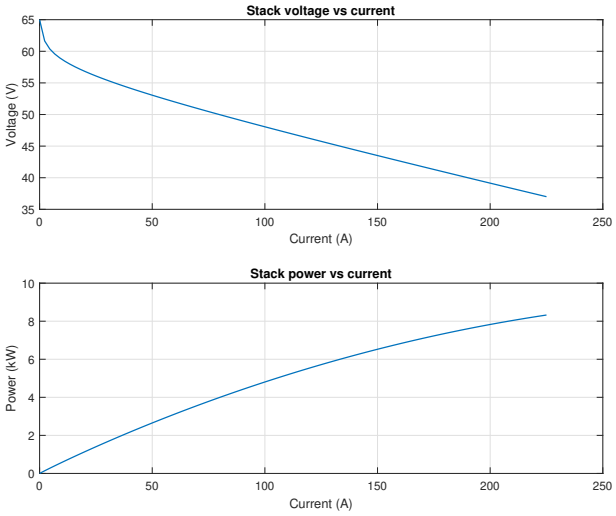

Fig. 2: Fuel Cell Stack characteristic curves

III. Neural Network Data-Driven Models

As it can be seen in previous section, the physical equations describing the behavior of the PEMFC are complicated and include many approximations for simplification. Using these equations inside NMPC for the PEFC model is computationally expensive and even inaccurate in some cases, hence the data-based algorithms for modeling the PEMFC are introduced as an alternative approach. This section introduces the process of collecting a proper data from the system and designing the data-driven models based on them.

A. Data collection

The machine learning algorithms rely on the input and output data of the system for modeling which represents a regression problem. This dataset should be comprehensive and be able to describe all the dynamics and working conditions of the system with sufficient resolution. Thus, the system should be excited properly when the training dataset is being collected from the system. The Pseudo-Random Sequence (PRS) signal is a natural candidate for this process as it behaves similar to white noise that contains all frequencies monotonically which

makes it capable of exciting all the dynamics of the system [1]. Three inputs are applied including fuel flow rate, air flow rate, and fuel supply pressure. The two desired outputs are the stack voltage and fuel consumption. The input values are changed between the following ranges:

$$\begin{aligned} 35\ lpm \leq V_{fuel} \leq 85\ lpm \\ 300\ lpm \leq V_{air} \leq 500\ lpm \\ 1.2\ bar \leq P_{fuel} \leq 3\ bar \end{aligned} \tag{15}$$

Fig. 3 shows the recorded inputs and outputs of the PEMFC.

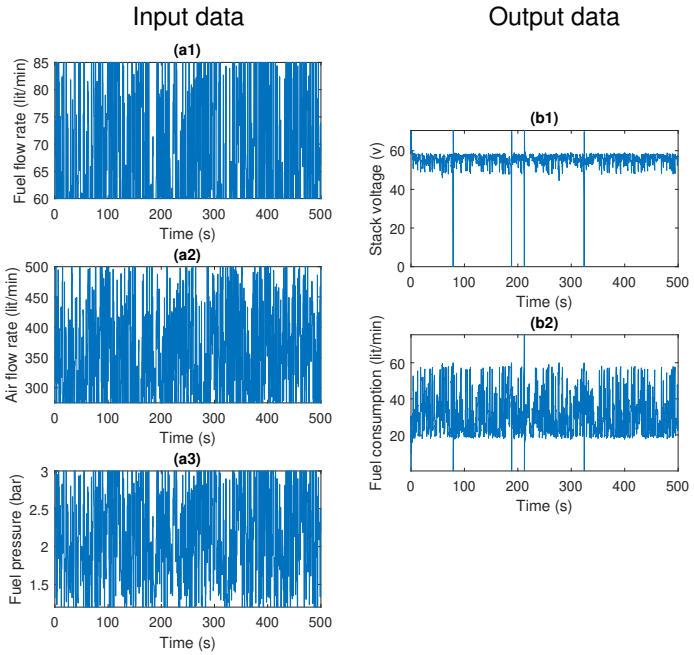

Fig. 3: PEMFC input and output data

This data set is then pre-processed in which the samples indicating the PEMFC shut-off modes are removed as only the steady state working condition is studied in this work.

B. PEMFC modeling

In order to obtain a regression model that maps the inputs to outputs with acceptable accuracy, different Neural Network (NN) architectures are utilized. These include shallow and deep Artificial Neural Networks (ANN) with and without feedback from the previous instances of outputs. In addition, the Recurrent Neural Network (RNN), Long Short-Term Memory (LSTM), and Gated Recurrent Unit (GRU) are selected for modeling since their architectures consider the dependencies between samples over time and can capture the dynamics of the system. Table II shows the Root-Mean-Squared Error (RMSE) of the stack voltage test data after these networks are trained with the best configuration in terms of the number of layers, neurons and activation functions. Based on these results, although all the approaches are able to model the data, the LSTM network offers the best performance with lowest possible RMSE.

TABLE II: RMSE of the trained models for predicting the stack voltage

Network architecture	RMSE
ANN without feedback	0.0588
ANN with feedback	0.0557
RNN	0.0523
LSTM	0.0506
GRU	0.0513

The LSTM network is one of common structures used for predicting time-series data. It allows capturing both short-term and long-term dependencies among samples. The selected configuration for the LSTM network consists of three layers, one fully-connected layer with 10 neurons and one LSTM layer with 5 cells and one output layer with two neurons. The prediction results of these two networks are shown in Fig. 4. Each LSTM neuron has two feedbacks, one from the short-term and the other one from the long-term memory. As a result, the total number of controlling states will be equal to 12 including 10 interior recurrent feedbacks plus 2 outputs of the system which are the fuel-cell voltage and hydrogen consumption.

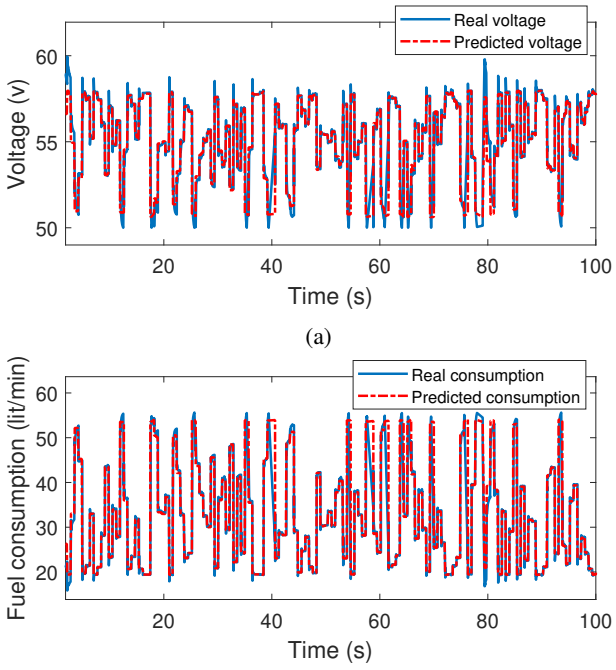

Fig. 4: Prediction results of the LSTM model for predicting: (a) Stack output voltage, (b) Stack fuel consumption rate

IV. NMPC BASED ON LSTM PREDICTION MODEL

Here, an NMPC is designed using the LSTM model from section III. The cost function for this system is derived in a quadratic form which ends up to a convex and smooth solution based on the system constraints [14]. The generated quadratic

cost function which is applied to the NMPC can be expressed as Eq. (16).

$$
\begin{aligned}
J(z_k) = {} & \Sigma_{i=0}^{N_p}\{W_1[V_{ref}(k+i|k) - V_{stack}(k+i|k)]\}^2 \\
& + \Sigma_{i=0}^{N_p}\{W_2[H_2Consumption(k+i|k)]\}^2 \\
& + \Sigma_{i=0}^{N_p-1}\{W_3[V_{fuel}(k+i|k)]\}^2 \\
& + \Sigma_{i=0}^{N_p-1}\{W_4[V_{air}(k+i|k)]\}^2 \\
& + \Sigma_{i=0}^{N_p-1}\{W_5[P_{fuel}(k+i|k)]\}^2 \\
& + \Sigma_{i=0}^{N_p-1}\{W_6[V_{fuel}(k+i|k) - V_{fuel}(k+i-1|k)]\}^2 \\
& + \Sigma_{i=0}^{N_p-1}\{W_7[V_{air}(k+i|k) - V_{air}(k+i-1|k)]\}^2 \\
& + \Sigma_{i=0}^{N_p-1}\{W_8[P_{fuel}(k+i|k) - P_{fuel}(k+i-1|k)]\}^2 \\
& + p_\epsilon \epsilon_k^2
\end{aligned}
\tag{16}
$$

In Eq. (16), the first term indicates the difference between the desired and actual values of the output voltage. The seconds term aims to minimize the amount of Hydrogen consumption as the fuel. The third, fourth, and fifth terms show the three inputs penalty costs which are fuel-flow-rate, air-flow-rate, and fuel supply pressure, respectively. The sixth, seventh, and eighth terms indicate the penalty costs related to the manipulated inputs move suppression, and the last term shows the violation effect of setting hard constraints on either inputs or output variables of the system. The prediction and controlling horizons of MPC are 20 seconds and 2 seconds, respectively. The sequential Quadratic Programming (SQP) was selected as the solver with the iteration number of 5000. Applied weights and constraints are as Eq. (17) and Eq. (18).

$$
\begin{aligned}
&\text{Input weights: } [w_3, w_4, w_5] = [1\ 0.1\ 10] \\
&\text{Output weights: } [w_1, w_2] = [500\ 10] \\
&\text{Inputs move suppression weights: } [w_6, w_7, w_8] = [1\ 1\ 1]
\end{aligned}
\tag{17}
$$

$$
\begin{aligned}
& 60\ lpm \leq V_{fuel} \leq 85\ lpm \\
& 275\ lpm \leq V_{air} \leq 500\ lpm \\
& 1.2\ bar \leq P_{fuel} \leq 3\ bar \\
& 50\ V \leq V_{stack} \leq 59\ V \\
& 16.1\ lpm \leq H_2Consumption \leq 58\ lpm
\end{aligned}
\tag{18}
$$

Based on the real NetStack-PS6 PEMFC model specifications [8], the fuel consumption variation range was determined as Eq. (18). To guarantee that the stack fuel consumption rate is not violated from the defined range, it was set as a hard constraint on the model. In this way, not only the fuel consumption is minimized based on the tracking reference, but also it will not exceed the selected limits at all.

V. Results and Discussions

For this part, by placing the LSTM prediction model inside the NMPC, the results for both step sequence and sinusoid voltage references are depicted in Fig. 5 and Fig. 6. The step sequence signal offers a typical reference tracking problem for PEMFC. The sinusoid reference is also studied as it contains

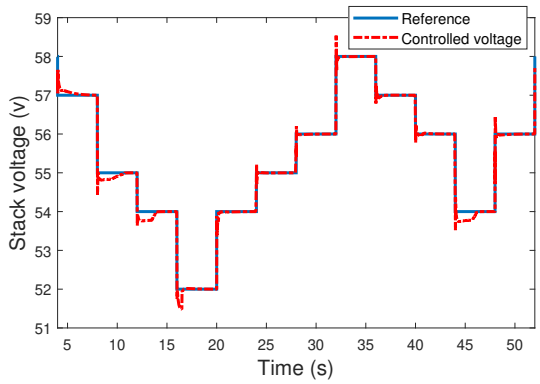

(a)

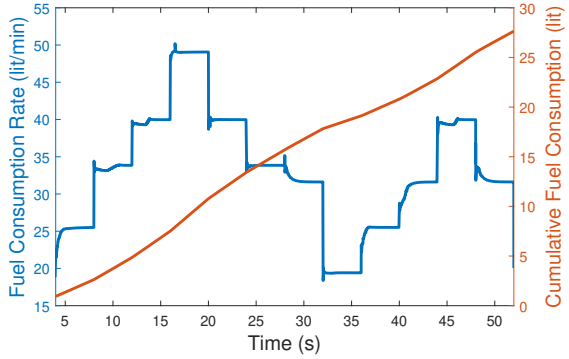

(b)

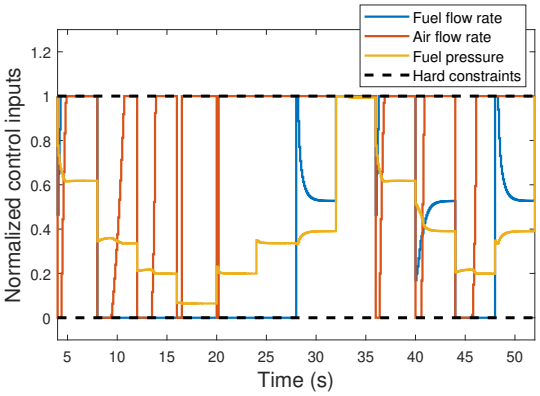

(c)

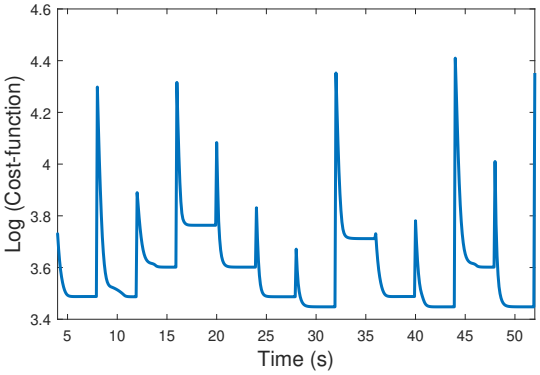

(d)

Fig. 5: Results with hard constraints and step reference. (a) Stack voltage tracking, (b) Reduced fuel consumption, (c) Normalized input signals, (d) Cost function

all continuous values in the valid range of output voltage and provides a second framework for validating the designed controllers.

It can be seen in Fig. 5a that a desirable voltage tracking has been achieved while the fuel consumption is being minimized in Fig. 5b. The total hydrogen fuel consumption of the system is 27.65 liters in this simulation. Based on Fig 5c, the manipulated variables are confined within the hard constraints and Fig. 5d shows the logarithm of the cost function value.

The similar procedure was repeated with sinusoid reference and the same results are recorded for this reference type as the step sequence reference which are shown in Fig. 6. Since this function is smoother comparing to the step sequence reference and has no abrupt changes, the output voltage in Fig. 6a follows the desired values more accurately. The total hydrogen consumption for the sinusoid reference is 35.70 liters during the a 52 seconds simulation as shown in 6b. The confined normalized control efforts and the cost function are depicted in Fig. 6c and 6d, respectively.

The results for these two simulation are summarized in Table III. The first two rows show the results for a linear MPC designed using an Auto-Regressive Exogenous (ARX) as the prediction model. Because of the non-linearity of the system, the ARX is not able to model the output voltage of the system properly. Hence, the voltage tracking error of this approach is too high that cannot be acceptable. However, the lower run time of this simple method comparing to other cases where the LSTM-NMPC is used shows the high computational cost of the proposed method due to the LSTM predictions. On the other hand, the RMSE of voltage tracking for LSTM-NMPC is considerably low which shows the efficiency of this method. The next two rows represent the case in which the fuel consumption is not controlled for the step sequence and sinusoid references. Comparing the total fuel consumption with the final two rows that a penalty to the amount of consumed fuel is added shows a 2.54 and 2.21 liters reduction in the total fuel consumption for the two types of references during a simulation of 52 seconds. This shows the effectiveness of considering the associated term in the cost function. The PEMFC studied in this paper can be classified as a secondary (urgent) power source based on the rated power which is 6 kW [9]. The average operating time of an urgent power plant is far longer than 52 seconds and the calculated fuel consumption reduction over 52 seconds can be extended to the longer time periods, leading to a considerable reduction in total fuel consumption.

VI. Conclusions

In this paper, machine learning model predictive control (ML-MPC) is used to adjust the fuel-cell output voltage and reduce hydrogen consumption using fuel flow rate, air flow rate, and fuel supply pressure as the controlling inputs. In this control approach, an LSTM network is trained to capture the behavior of a 6 kW fuel-cell system including a 100V-dc power generating circuit. The obtained data-driven model is then placed inside the MPC controller as the prediction

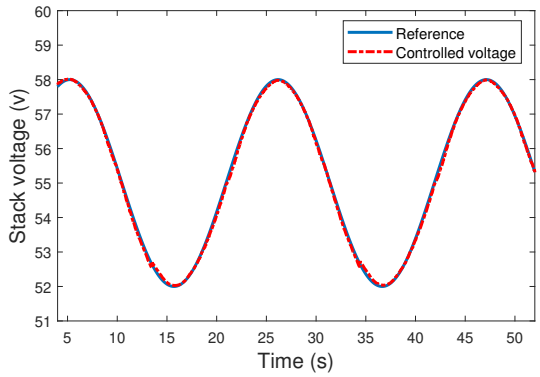

(a)

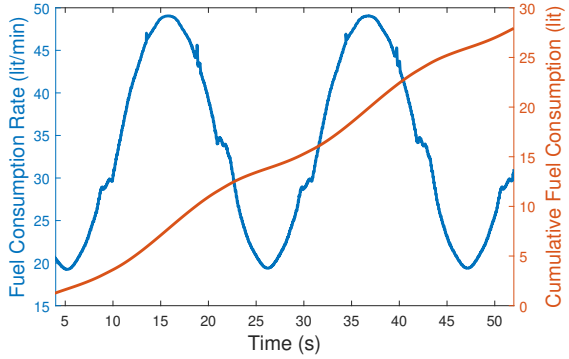

(b)

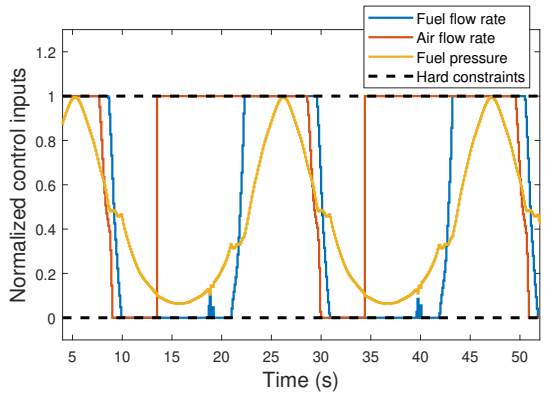

(c)

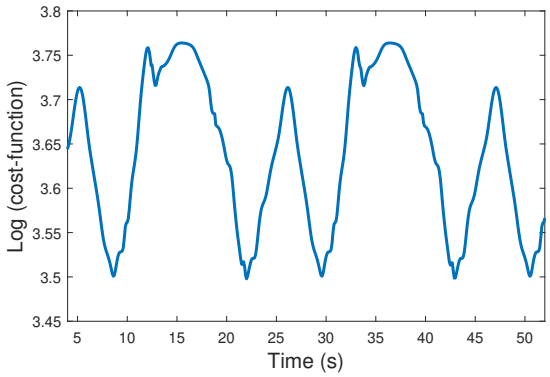

(d)

Fig. 6: Results with hard constraints and sinusoid reference tracking. (a) Stack voltage tracking, (b) Reduced fuel consumption, (c) Normalized input signals, (d) Cost function

TABLE III: Results of the designed controllers

Case study	RMSE (volt)	Fuel consumption (L)	Run time (s)
Linear MPC with step voltage reference	1.34	29.44	7.3
Linear MPC with sinusoid voltage reference	1.74	31.93	8.3
LSTM-NMPC with step voltage reference without fuel consumption minimization	0.1259	30.19	388.24
LSTM-NMPC with sinusoid voltage reference without fuel consumption minimization	0.2328	30.14	469.46
LSTM-NMPC with step voltage reference with fuel consumption minimization	0.1036	27.65	353.45
LSTM-NMPC with sinusoid voltage reference with fuel consumption minimization	0.0645	27.93	439.35

model instead of using highly nonlinear control oriented state equations of the system. The results show that the voltage tracking task as well as the fuel consumption reduction are being accomplished properly. In addition, the hard constraints are not violated during the simulation. Overall, this study demonstrates that combining ML modeling methods with MPC is a promising approach for controlling PEMFC.

ACKNOWLEDGMENT

The authors of this paper acknowledge Mohamad Ali Tofigh for his comments during the course of the study.

REFERENCES

[1] W. Ming, P. Sun, Z. Zhang, W. Qiu, J. Du, X. Li, Y. Zhang, G. Zhang, K. Liu, Y. Wang, *et al.*, "A systematic review of machine learning methods applied to fuel cells in performance evaluation, durability prediction, and application monitoring," *International Journal of Hydrogen Energy*, 2022.

[2] W. Daud, R. Rosli, E. Majlan, S. Hamid, R. Mohamed, and T. Husaini, "PEM fuel cell system control: A review," *Renewable Energy*, vol. 113, pp. 620–638, 2017.

[3] A. C. Fărcaş and P. Dobra, "Adaptive control of membrane conductivity of pem fuel cell," *Procedia Technology*, vol. 12, pp. 42–49, 2014.

[4] R. Methekar, V. Prasad, and R. Gudi, "Dynamic analysis and linear control strategies for proton exchange membrane fuel cell using a distributed parameter model," *Journal of Power Sources*, vol. 165, no. 1, pp. 152–170, 2007.

[5] J. T. Pukrushpan, A. G. Stefanopoulou, S. Varigonda, L. M. Pedersen, S. Ghosh, and H. Peng, "Control of natural gas catalytic partial oxidation for hydrogen generation in fuel cell applications," *IEEE Transactions on Control Systems Technology*, vol. 13, no. 1, pp. 3–14, 2004.

[6] W. Garcia-Gabin, F. Dorado, and C. Bordons, "Real-time implementation of a sliding mode controller for air supply on a PEM fuel cell," *Journal of Process Control*, vol. 20, no. 3, pp. 325–336, 2010.

[7] N. Chatrattanawet, T. Hakhen, S. Kheawhom, and A. Arpornwichanop, "Control structure design and robust model predictive control for controlling a proton exchange membrane fuel cell," *Journal of Cleaner Production*, vol. 148, pp. 934–947, 2017.

[8] C. Bordons, A. Arce, and A. Del Real, "Constrained predictive control strategies for PEM fuel cells," in *2006 American Control Conference*, pp. 6–pp, IEEE, 2006.

[9] S. N. Motapon, O. Tremblay, and L.-A. Dessaint, "Development of a generic fuel cell model: application to a fuel cell vehicle simulation," *International Journal of Power Electronics*, vol. 4, no. 6, pp. 505–522, 2012.

[10] A. Norouzi, H. Heidarifar, M. Shahbakhti, C. R. Koch, and H. Borhan, "Model predictive control of internal combustion engines: A review and future directions," *Energies*, vol. 14, no. 19, p. 6251, 2021.

[11] Z. Ural, M. T. Gencoglu, and B. Gumus, "Dynamic simulation of a pem fuel cell system," in *Proceedings of 2nd International Hydrogen Energy Congress and Exhibition*, pp. 1–12, 2007.

[12] L. Fan, J. Zhang, and C. Li, "Model predictive control on constant voltage output of a proton exchange membrane fuel cell," *Journal of Engineering Science and Technology Review*, vol. 6, no. 2, pp. 115–119, 2013.

[13] O. Tremblay, L.-A. Dessaint, and N. Souleman, "A generic fuel cell model for the simulation of fuel cell vehicles," in *2009 IEEE vehicle power and propulsion conference*, pp. 1722–1729, IEEE, 2009.

[14] S. Moghadasi, A. K. Anaraki, A. Taghavipour, and A. H. Shamekhi, "Real-time nonlinear model predictive energy management system for a fuel-cell hybrid vehicle," *Journal of the Brazilian Society of Mechanical Sciences and Engineering*, vol. 41, no. 10, p. 457, 2019.